

**COMPARTMENT BASED POPULATION BALANCE
MODEL DEVELOPMENT AND VALIDATION OF A
HIGH SHEAR WET GRANULATION PROCESS VIA
DRY BINDER ADDITION**

BY CHANDRA KANTH BANDI

**A thesis submitted to the
Graduate School—New Brunswick
Rutgers, The State University of New Jersey
in partial fulfillment of the requirements
for the degree of
Master of Science
Graduate Program in Chemical and Biochemical Engineering**

**Written under the direction of
Dr. Rohit Ramachandran
and approved by**

New Brunswick, New Jersey

October, 2016

ABSTRACT OF THE THESIS

Compartment based population balance model development and validation of a high shear wet granulation process via dry binder addition

by Chandra Kanth Bandi

Thesis Director: Dr. Rohit Ramachandran

The addition of binder to facilitate the granulation in high shear wet granulation (HSWG) process can be achieved either by adding a binder liquid with uniform viscosity and binder content (wet binder addition) or by adding a liquid to the pre-mixed mixture of solid binder and aggregating granules, that dissolves the binder enabling varying viscosity (dry binder addition). Population balance modeling has been used traditionally to model the wet binder addition (WBA) systems. However, these models solely cannot represent the dry binder addition (DBA) systems which includes an additional process of dissolution of binder in liquid. In this work, a reduced ordered compartment based population balance model (PBM) integrated with particle dissolution model was developed to address the differences in particle size distribution obtained from dry and wet binder addition granulation. The experimental data for the HSWG process using WAB and DBA was obtained from Bristol-Myers-Squibb. The data was used to estimate the kernel parameters to validate the integrated model to be used as predictive tool. This model showed good agreements with experimental data in capturing the trends in mean particle size.

Acknowledgements

Thank you Mother and Father

I would like to express my sincere gratitude to my thesis adviser, Dr. Rohit Ramachandran who was instrumental in guiding and supporting me through this work. I would like to thank my advisory committee members Dr. Ravendra Singh and Dr. Gerardo Callegari for their time and suggestions. I would like to extend my heartfelt appreciation to Anik Chaturbedi, Dheeraj Reddy and Anwesha Chaudhury who have helped me at various stages of my project and without whom the completion would have been challenging. Special thanks to Dr. Dana Barsasso who helped me learn the modeling techniques used for my project.

I am greatly indebted to the Ashu Tamrakar, Dr. Savitha Panikar, Pallavi Pawar and Sarang Oka who made my work in CBE wonderful and comfortable. It was my pleasure to work alongside my colleagues Sreenath Yeluri, Suparna Rao, Subhodh Karkala and Manogna Adepu.

Lastly, I thank Bristol-Myers-Squibb for sponsoring the project and providing the experimental data required to complete my work.

Table of Contents

Abstract	ii
Acknowledgements	iii
List of Tables	vi
List of Figures	vii
1. Introduction	1
1.1. Objectives	2
2. Background	3
2.1. Wet Granulation and Binder Addition Types	3
2.2. Compartment Based Population Balance Modeling	4
2.3. Model Reduction	5
3. Experimental Procedure	7
3.1. Materials and Methods	7
3.2. Physical characterization of granules	7
4. Mathematical model development	9
4.1. Compartment Based PBM	9
4.1.1. Aggregation	11
4.1.2. Breakage	12
4.1.3. Liquid addition and consolidation	13
4.1.4. Circulation	13
4.2. Dissolution Model	14
4.3. Integration of Compartment and Dissolution Model	15

4.4. Drop Penetration	17
4.5. Numerical Methods	17
5. Results and Discussion	20
5.1. Granule growth in Dry & Wet HPC addition	20
5.2. Granule growth in Dry & Wet PVP addition	23
5.3. Sensitivity Analysis	26
5.4. Prediction of wet binder addition from dry binder addition	27
6. Conclusion	29

List of Tables

3.1. Operating conditions of the wet granulation process	7
4.1. Process parameters, material properties used in simulation	16
4.2. Process parameters, material properties used in simulation	18
5.1. Sum of squared errors in the model predicted average diameter for the estimated parameters	28

List of Figures

2.1. Schematic showing formulation of two compartments in a granulator	5
4.1. Figure showing spray zone and bulk zones of dry binder and wet binder addition systems. μ_2 and μ_3 represent the viscosity in spray zone and bulk zone of dry binder system respectively while μ_1 is the viscosity of both compartments in wet binder system	10
4.2. Dissolution of Binder Particle under non-sink conditions	15
4.3. Integration of 1-D PBM and Dissolution Model using a viscosity calibration model	16
5.1. Conservation of total solid and liquid volumes over time	20
5.2. Variation of binder solution concentration with time for HPC in spray zone and bulk zone	22
5.3. Experimental & model predicted average diameter for wet & dry addition of HPC	23
5.4. Correlation of viscosity with binder concentration in water	24
5.5. Variation of binder solution concentration with time for PVP in spray zone and bulk zone	24
5.6. Experimental & model predicted average diameter for wet & dry addition of PVP	25
5.7. Prediction of wet binder addition by calibrating the model with dry binder addition	27

Chapter 1

Introduction

Granulation is a process of enlargement of fine particles into large agglomerates to improve the particle flowability and compressibility [31] due to which it is considered as one of the key unit operation in various particulate industries manufacturing pharmaceuticals, agricultural chemicals, minerals and detergents. In the pharmaceutical industry, granulation is majorly used for the production of solid dosage forms such as tablets and capsules. Owing to its economic importance, many ground breaking theories and wide research has been done in understanding the process. However, in spite of the decades of research many industrial plants operate at lower efficiency due to poor understanding and control [16]. Also, the U.S. Food and Drug Administration (FDA) has mandated the implementation of Quality by Design (QbD) approach in the pharmaceutical manufacturing process. This has increased the demand for a better understanding of the granulation, one of the key unit of manufacturing processes to facilitate process control and product quality [4]. A systems approach entailing mathematical modeling allows the researchers to optimize and control the granulation process [6].

Mathematical modeling of wet granulation process using population balance models (PBM) is a well accepted technique in scientific community. The discrete nature of population balance equations which can capture the rate mechanisms provides significance advantage over other modeling approaches. Many one dimensional models have been established but the limitations of these models reported by Iveson [16] has demanded for the need of more accurate multidimensional model. Therefore, a volume based three dimensional (3D) PBM was proposed by Verkoeijen et al. [34] and applied to a wet granulation process by Darelus et al. [11]. In this approach, the volume of particle

is divided into three independent particle parameters which can measure different particle properties such as porosity, moisture content, pore saturation. The independent parameters are volume of solid s , volume of liquid l , volume of gas g of a single particle. Furthermore, development of predictive mechanistic breakage and aggregation kernels has given better insight and control of these mechanisms.

Wet granulation is a process in which the binder liquid plays a major role in determining the rates of processes such as aggregation and breakage and it significantly affects the final particle size distribution. This binder liquid can be introduced into the system by adding either a liquid binder of uniform viscosity or a pure liquid to the dry binder present in the system. Unlike the former method of binder addition for which various mathematical models have been developed, the dry binder addition system has not been computationally studied till date. In this study, we present a compartment based population balance model accounting for a spray and bulk zone of different viscosity and exchange of particles and liquid between the zones. We also account for a binder dissolution sub-model that computes the rate of dissolution of binder in water that subsequently governs the increase of viscosity in the system and the corresponding aggregation and breakage rates. Results show that the developed model can capture experimental trends of differences in particle growth rates for dry binder addition compared to wet binder addition.

1.1 Objectives

The purpose of this study was to develop a PBM model for both cases of wet granulation processes with the following objectives,

1. Develop an integrated compartmental PBM with binder dissolution sub-model for granulation process with dry binder addition.
2. Validate the model for both WBA and DBA with different materials of binders.

Chapter 2

Background

2.1 Wet Granulation and Binder Addition Types

Wet granulation involves addition of a liquid solution (with or without binder) to form a wet mass which further generates granules of varying sizes depending on process parameters. Initially, the dry porous particles are uniformly mixed and when liquid gets added, it fills the pores and wets the dry granules. Wet granulation involves three sets of rate process (a.) Wetting and nucleation b.) Consolidation and growth c.) Attrition and breakage [17]. Wetting and Nucleation are the first and critical steps of the wet granulation where the liquid binder added to the system comes in contact with granules to form nuclei. Later on, these nuclei collide with each other and equipment walls leading to granule compaction by squeezing the air trapped inside the nuclei. During this step, fine particle coalesce to form bigger granules. Breakage and attrition takes place in these high shear granulators controlling the granule growth and achieving desired particle size distribution.

The system involving the two different methods of liquid binder addition can be classified as follows, a.) Pure liquid and solid binder is pre-mixed before addition to the granulator containing API and excipient termed as *wet binder addition* (WBA). b.) Pure liquid is added to the granulator containing solid binder and API termed as *dry binder addition* (DBA). While the WBA is a conventional method of addition, dry binder addition systems are very efficient in the case of high viscosity systems. A highly viscous binder would impart difficulties during liquid addition by spraying. In the DBA system, the solid binder and aggregating granules are pre-blended before the addition of a dissolving less viscous liquid. The liquid addition wets the surfaces of

all particles thus simultaneously saturating the granule pores and dissolving the binder which will facilitate aggregation. However, the partition ratio of liquid for binder particles and granules is complex and needs thorough understanding and validation using experiments. The dissolution of binder in liquid begins the aggregation and breakage process where granules collide among themselves changing their size. Alongside these process, while consolidation leads to compaction, it also enhances the amount of surface liquid used for aggregation contributing to granule growth. All these rate processes depend on various process parameters such as diameter and rpm of impeller, liquid spray rate, composition of mixture and material properties such as viscosity of binder liquid, contact angle between binder liquid and granule, coefficient of restitution between granule and granulator walls and among granules, and granule porosity. The effect of these parameters on granule growth has been studied traditionally in a HSWG for the wet binder addition. Hence, a need for the study of these parameters on dry binder granulation exists.

2.2 Compartment Based Population Balance Modeling

The modeling of the wet granulation system has been done using various approaches such as Population Balance Modeling (PBM) ([16],[10],[11]), Discrete Element Modeling (DEM) ([28]) and Hybrid PBM-DEM modeling ([2], [3], [19]). The modeling of granulation started with application of 1D PBMs [23] and further extending to various multi-dimensional PBM due to the limitations of 1D model in terms of their application to only one intrinsic property of the granules. The 1D models showed inadequacy to be applied to the complex rate mechanism occurring during the process and determining other properties such as porosity, binder content. Later on, the developed multidimensional models studied the granulation systems based on the assumption that the granulator behaves as a well mixed system. While this assumption holds good for some ideal system, existence of inhomogeneities in a system cannot be ignored. The wetting of particles during liquid addition can be studied as either using a drop controlled regime or a mechanical dispersion regime [13]. The occurrence of drop controlled regime where one liquid droplet can wet only one particle makes the system homogeneous but

is very limited. In other case, mechanical dispersion regime considers the wetting of multiple particles by a single droplet which resembles the mechanistic system conditions. However, this imparts inhomogeneity to the system and cannot be studied using a single compartment PBM. The particles that are more wetted with liquid have increased nucleation and aggregation when compared to those containing less liquid and it leads to the formation of a wider distribution of granules. Hence, application of a model using multiple compartments to address the heterogeneity has found huge significance in pharmaceutical process modeling. The multi-compartment model employs various compartments to define certain homogeneous regions in the granulator and its information is used to develop a PBM for each individual compartment. In addition, the movement of particles between compartments is quantified using a Markov-chain approach [9]. The multi-compartment models have been successfully applied to systems such as particle coating and layered granulation [22] and fluid bed granulation [24].

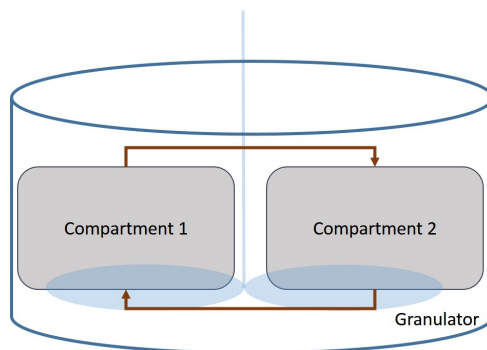


Figure 2.1: Schematic showing formulation of two compartments in a granulator

2.3 Model Reduction

The higher ordered models along with various mechanistic rate kernels are very useful in accounting for heterogeneity, integrating process parameters and material properties with the process rates and final granule properties. However, these models are computationally expensive and are not desired for process design and analysis which demands for the development of a computationally less intensive lumped model. Biggs et al. [5], Hounslow et al. [14] illustrated that a higher dimension model can be reduced to a lower

dimension to decrease the computation time and complexity. Reduced order model simplify the solution of model where one or more granule characteristics are lumped into remaining distributions. Barrasso and Ramachandran [1] studied reduction of a four dimensional model comprising of solid, liquid, gas and granule composition dimensions to 3D model, 2D model and 1D model. A significant reduction of 95 % in computational time was observed with reduction from a 4-D model to 3-D model without much change in the prediction of final granule properties.

Chapter 3

Experimental Procedure

3.1 Materials and Methods

Microcrystalline cellulose (MCC), (FMC Co., Philadelphia, PA) was granulated with binder dissolved in water in a 10-liter PMA high shear granulator in case of wet binder addition. The binders used for this study were HPC EXF and PVP K29/32 obtained from Ashland Specialty Ingredients, Wilmington, DE. The granulation was performed on a batch size of 1664 g with 96% of MCC and 4% binder. For dry binder addition, the binder particles were mixed with MCC prior to granulation and water was added to this mixture during liquid addition stage. These experiments were conducted at Bristol-Myers Squibb, New Brunswick, NJ, USA. The operating conditions for the granulation process can be found in Table 3.1.

Table 3.1: Operating conditions of the wet granulation process

Parameter	Value
Mixing speed	306 rpm
Dry mixing time	4 min
Liquid spray rate	400 g/min
Liquid addition time	3 min
Wet massing time	15 min

3.2 Physical characterization of granules

The particle size distribution of the dried granules was measured by sieve analysis using an Allen Bradley Sonic Sifter (Allen Bradley, Milwaukee, WI) equipped with a set of 6 screens and pan. The screens used in this case were US 30 (590 μm), 40 (420 μm),

60 (250 μm), 80 (180 μm), 140 (106 μm) and 270-mesh (53 μm). Bulk density was measured using a 100 cc cylinder.

Chapter 4

Mathematical model development

4.1 Compartment Based PBM

Multi-compartment population balance modeling has been used to address the inhomogeneity in various systems such as fluid bed coating [27], crystallization process [25], layered granulation [22], drum granulation [30]. The dry binder addition granulation is non-homogeneous in terms of viscosity and liquid content and application of compartment based modeling helps in understanding this system. In dry binder addition system, the liquid is unequally distributed with the majority of liquid present at the proximity of spray zone and less liquid towards the far end which imparts heterogeneity. For the process of model development, the system is divided into two compartments, based on the viscosity and liquid amount; Spray zone and Bulk zone. The areas with more liquid and less binder come under spray zone while the bulk zone has areas with less liquid and more binder and particles as can be illustrated in Figure 4.1. Both compartments have differences in viscosity, amount of liquid, number of particles and are modeled separately using a 1-D PBM. Use of lumped 1-D PBM has its advantages over higher dimensional PBM in terms of lower computational power and time with minor accuracy losses [1]. Therefore, the liquid and gas volumes are lumped into the solid granule volume and a lumped 1-D PBM for each compartment is developed as follows.

PBM for compartment 1 (spray zone):

$$\frac{\partial F_1(s_1, t)}{\partial t} = R_{1,agg} + R_{1,break} - \left(R_{circulation} \left(\frac{F_1(s_1, t)}{\alpha_1} - \frac{F_2(s_2, t)}{\alpha_2} \right) \right) \quad (4.1)$$

$$\frac{\partial L_1(s_1, t)}{\partial t} = F_1(s_1, t) \frac{dl_1}{dt} + R_{1,agg,liq} + R_{1,break,liq} \quad (4.2)$$

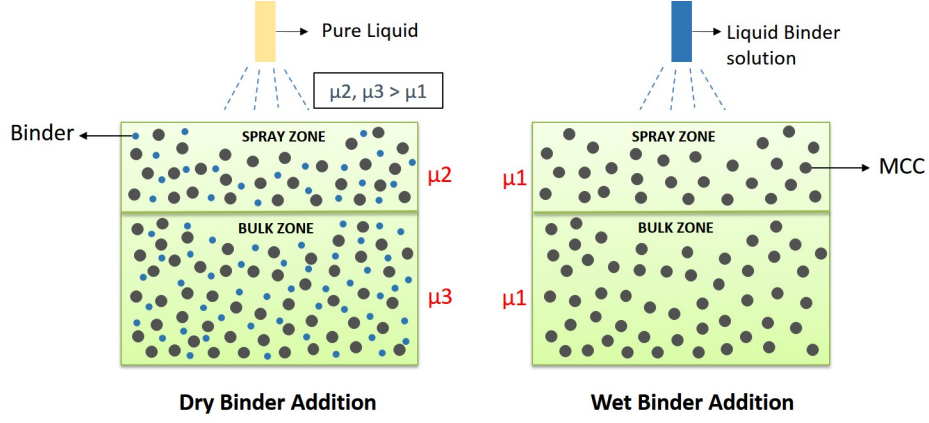


Figure 4.1: Figure showing spray zone and bulk zones of dry binder and wet binder addition systems. μ_2 and μ_3 represent the viscosity in spray zone and bulk zone of dry binder system respectively while μ_1 is the viscosity of both compartments in wet binder system

$$\frac{\partial G_1(s_1, t)}{\partial t} = F_1(s_1, t) \frac{dg_1}{dt} + R_{1,agg,gas} + R_{1,break,gas} \quad (4.3)$$

PBM for compartment 2 (bulk zone):

$$\frac{\partial F_2(s_2, t)}{\partial t} = R_{2,agg} + R_{2,break} - \left(R_{circulation} \left(\frac{F_2(s_2, t)}{\alpha_2} - \frac{F_1(s_1, t)}{\alpha_1} \right) \right) \quad (4.4)$$

$$\frac{\partial L_2(s_2, t)}{\partial t} = F_2(s_2, t) \frac{dl_2}{dt} + R_{2,agg,liq} + R_{2,break,liq} \quad (4.5)$$

$$\frac{\partial G_2(s_2, t)}{\partial t} = F_2(s_2, t) \frac{dg_2}{dt} + R_{2,agg,gas} + R_{2,break,gas} \quad (4.6)$$

Here, s_x , l_x , g_x represents the solid, liquid and gas volumes of granule in respective compartments where $x=1$ or 2 indicating spray zone and bulk zone accordingly. $L_x(s_x, t) = l_x * F_x(s_x, t)$ and $G_x(s_x, t) = g_x * F_x(s_x, t)$ is the total liquid volume and gas volume respectively present in the bin s_x . The terms α_1 and α_2 correspondingly represents the volume ratio associated with spray zone and bulk zone and its values are found in Table 4.2

4.1.1 Aggregation

$R_{x,agg}$ in Equation 4.1 represents the net rate of formation and depletion of granules in each bin. $R_{x,agg,liq}$ and $R_{x,agg,gas}$ transfer total amount of liquid and gas contained in aggregating particles to final granule bin. As described in Equations 4.8 and 4.9, these rates can be evaluated using appropriate kernels. Several empirical kernels ([26],[33]) and semi-mechanistic kernels ([8],[15]) have been proposed in the literature which characterizes this rate mechanism. With respect to reflecting the effect of operating and material parameters on the process, mechanistic kernels have advantage over empirical kernels.

The net rate of aggregation consists of rate of formation of larger granules ($R_{x,agg}^{form}$) and rate of depletion of smaller granules ($R_{x,agg}^{dep}$).

$$R_{x,agg}(s_x, t) = R_{x,agg}^{form}(s_x, t) - R_{x,agg}^{dep}(s_x, t) \quad (4.7)$$

$$R_{x,agg}^{form}(s_x, t) = \frac{1}{2} \int_0^{s_x} \beta(s_x - s'_x, s'_x) * F(s_x - s'_x, t) * F(s'_x, t) ds'_x \quad (4.8)$$

$$R_{x,agg}^{dep}(s_x, t) = F(s_x, t) * \int_0^{S_{max}-s_x} \beta_{agg}(s_x, s'_x) F(s'_x, t) ds_x \quad (4.9)$$

Similarly, the $R_{x,agg,liq}$, $R_{x,agg,gas}$ can be defined as in Equations 4.10 and 4.11 respectively

$$R_{x,agg,liq} = \frac{1}{2} \int_0^{s_x} \beta(s_x - s'_x, s'_x) * F(s_x - s'_x, t) * F(s'_x, t) * (l_x(s_x - s'_x, t) + l_x(s'_x, t)) ds'_x - L_x(s_x, t) \int_0^{S_{max}-s_x} \beta(s_x, s'_x, t) F(s'_x, t) ds_x \quad (4.10)$$

$$R_{x,agg,gas} = \frac{1}{2} \int_0^{s_x} \beta(s_x - s'_x, s'_x) * F(s_x - s'_x, t) * F(s'_x, t) * (g_x(s_x - s'_x, t) + g_x(s'_x, t)) ds'_x - G_x(s_x, t) \int_0^{S_{max}-s_x} \beta(s_x, s'_x, t) F(s'_x, t) ds_x \quad (4.11)$$

where s_x , l_x , g_x are the solid volume, liquid volume and gas associated with a granule and x can be 1 or 2 indicating spray zone or bulk zone. A semi-mechanistic aggregation kernel β is evaluated using Equation 4.12 defined by Chaudhury et al. [8]

$$\beta_{agg} = fn(\beta_0, \mu, F, rpm, V_{surface}, \rho_{solid}, \theta) \quad (4.12)$$

4.1.2 Breakage

Breakage occurs when granules disintegrate into two or more granules. The rate of formation of smaller particles ($R_{x,agg}^{form}$) and rate of depletion of larger particles ($R_{x,agg}^{dep}$) are incorporated into net rate of breakage ($R_{x,agg}$) which are defined in the following equations.

$$R_{x,break}(s_x, l_x, g_x, t) = R_{x,break}^{form}(s_x, l_x, g_x, t) - R_{x,break}^{dep}(s_x, l_x, g_x, t) \quad (4.13)$$

$$R_{x,break}^{form}(s_x, t) = \int_{s_x}^{S_{max}} K_{break}(s'_x) b(s'_x, s_x) * F(s'_x, t) ds'_x \quad (4.14)$$

$$R_{x,break}^{dep}(s_x, t) = K_{break}(s_x) F(s_x, t) \quad (4.15)$$

Similarly, the $R_{x,break,liq}$, $R_{x,break,gas}$ which accounts for volumes of liquid and gas transferred due to breakage can be defined as in Equations 4.16 and 4.17 respectively

$$R_{x,break,liq} = V(s_x, t) \int_{s_x}^{S_{max}} K_{break}(s'_x) b(s'_x, s_x) * \frac{L(s'_x, t)}{V(s'_x, t)} ds'_x - K_{break}(s_x) L(s_x, t) \quad (4.16)$$

$$R_{x,break,gas} = V(s_x, t) \int_{s_x}^{S_{max}} K_{break}(s'_x) b(s'_x, s_x) * \frac{G(s'_x, t)}{V(s'_x, t)} ds'_x - K_{break}(s_x) G(s_x, t) \quad (4.17)$$

Here, $V(s_x, t)$ is the total volume associated with each particle in bin s_x and $x = 1$ or 2 to represent the compartments. A semi-empirical breakage kernel K_{break} is evaluated using Equation 4.18 as defined in K.A. Kusters [18] and Soos et al. [32]

$$K_{break} = \left(\frac{4}{15\pi} \right)^{1/2} G_{shear} \exp \left(- \frac{B}{G_{shear}^2 R(s_x)} \right) \quad (4.18)$$

where, G_{shear} is the shear velocity which is formulated as $G_{shear} = \frac{\pi}{60} * D_{imp} * rpm$ and B is the breakage parameter and $R(s_x)$ is radius of the granule that undergoes breakage.

4.1.3 Liquid addition and consolidation

The terms $\partial l / \partial t$ and $\partial g / \partial t$ respectively represent the liquid addition rate and consolidation rate for each granule in the model. Liquid addition process enhances the aggregation rate while the consolidation is the decrease in particle porosity due to compaction of particles. Consolidation is represented as exponential decay of porosity [34] in terms of minimum granule porosity ϵ_{min} and rate constant (c) as shown in Equation 4.20. The granule porosity is expressed in Equation 4.19.

$$\epsilon(s_x, l_x, g_x) = \frac{l_x + g_x}{s_x + l_x + g_x} \quad (4.19)$$

$$\frac{dg}{dt} = -c \frac{(s_x + l_x + g_x)(1 - \epsilon_{min})}{s_x} \left[l_x - \frac{\epsilon_{min}(s_x)}{1 - \epsilon_{min}} + g_x \right] \quad (4.20)$$

The liquid is sprayed at a specific rate U_{spray} on the granules which facilitates the aggregation. The amount of liquid received by each particle depends on its solid volume and is indicated in Equation 4.21

$$\frac{dl}{dt} = \frac{U_{spray} * s_x}{\int_0^{s_x} F(s_x, t) * s_x} \quad (4.21)$$

4.1.4 Circulation

Each compartment is modeled individually using a lumped 1-D PBM. However, both compartments belong to the same system and hence an interaction between both systems is necessary. The particles in each compartment are exchanged based on the circulation rate between the spray and bulk zones defined in Equation 4.22. The particles that are exchanged include granules, external liquid and dry binder (in case of

DBA) and this exchange facilitates the homogenization of the system after a certain time period. The movement of particles within the system depends on the viscosity which is dynamic in the case of dry binder addition system, therefore the circulation rate should depend on viscosity. However, in this work, the circulation rate is assumed to be constant.

$$R_{circulation} = K * rpm \quad (4.22)$$

where K is circulation rate factor assumed to be constant.

4.2 Dissolution Model

In the dry binder addition granulation, the binder is premixed with Micro Crystalline Cellulose (MCC) and liquid is sprayed into the system. During the liquid addition, a certain amount of liquid enters the porous MCC while the remaining liquid dissolves the binder. The dissolution mechanism and rate profile can be studied with the help of work done by Wang and Flanagan [35]. The authors have developed a general solution for dissolution of sphere under sink and non-sink conditions using a diffusion layer model. When the dissolving liquid volume is at least 3 times higher than the volume required for saturation, sink conditions exist. On the other hand, if the liquid volume is less than the saturation volume, it is termed as non-sink conditions. Unlike sink conditions, the bulk concentration of particles in liquid in non-sink condition is not zero which affects the dissolution rate. At the early stages of liquid addition, the amount of liquid is not sufficient to dissolve the total binder present in the system and hence non-sink conditions are assumed. A general solution of the dissolution of spherical particles under non-sink conditions can be obtained from the work done by Wang and Flanagan [35]. The binder particles are assumed to be spherical and the dissolution of spherical binder is assumed to occur radially through diffusion which can be shown in Figure 4.2. With the further assumption that all the binder particles are in contact with the liquid present in the respective compartments and diffuse simultaneously, the following dissolution model was developed. The amount of binder dissolved for a particular time

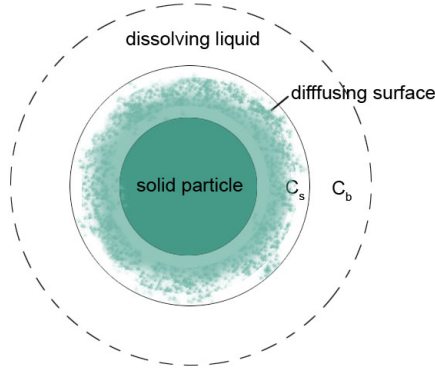


Figure 4.2: Dissolution of Binder Particle under non-sink conditions

is calculated using the Equation 4.23 which can be used to evaluate the viscosity of the system.

$$\frac{dA_i}{dt} = \frac{-D * (C_s - C_b) * (A_i + h_i)}{\rho * h_i * A_i} \quad (4.23)$$

$$C_b = \frac{4 * \pi * ((A_{init})^3 - (A_i)^3) * \rho}{3 * V_{i,ext}} \quad (4.24)$$

Here, A_{init} and A_i is the radius of binder particle at initial time and time t respectively with density ρ . The binder diffuses into external liquid volume $V_{i,ext}$, using a diffusion layer of thickness h_i with a diffusion coefficient D . C_s and C_b is the maximum solubility concentration and bulk concentration of binder in liquid.

4.3 Integration of Compartment and Dissolution Model

The population balance model given by Equation 4.1 accounts for various processes occurring in the granulator and these processes are represented by rate kernels. Use of mechanistic kernels that depends on process parameters provides better understanding and control of the process. A semi-mechanistic kernel by Chaudhury et al. [8] used in the study depends majorly on viscosity of the system as shown in the Appendix. Unlike the case of WBA where the system viscosity is uniform, the DBA system has variable viscosity due to dissolution of binder. The external liquid due to pore saturation and consolidation is used for binder dissolution and can be calculated using the 1-D PBM equation. The dissolution model uses the external liquid volume to calculate the amount

Table 4.1: Process parameters, material properties used in simulation

Property / Parameter	Symbol	Model Value
Granulation time	t_{final}	1320 s
Volume of first bin, solid	s_1	$4.8 \times 10^{-13} m^3$
Total number of bins	ns	14
Volume ratio of spray zone	α_1	0.3
Volume ratio of bulk zone	α_2	0.7
Liquid spray rate	U_{spray}	$5 \times 10^{-6} m^3/s$
Aggregation constant	B_0	6.8×10^{-11}
Breakage constant	B	3.6×10^{-6}
Consolidation constant	c	3
Circulation rate constant	K	1×10^{-6}
Granule density	den_s	$350 Kg/m^3$
Minimum granule porosity	ϵ_{min}	0.3
Granule liquid saturation	x^*	0.23
Contact angle	θ	1.5 radian
HPC Binder diffusion coefficient	D	$8.3 \times 10^{-9} m^2/s$
Initial binder size	A_{init}	$49.375 \mu m$
Binder solubility	C_s	0.33
Diffusion layer	h_i	$0.5 \mu m$
Water density	den_l	$1000 Kg/m^3$

of binder dissolved which is further applied to calculate the viscosity of system based on the viscosity calibration model developed between dissolved binder percentage and viscosity. The viscosity is then used by aggregation kernel of 1-D PBM to predict the external liquid content and granule properties like diameter and porosity.

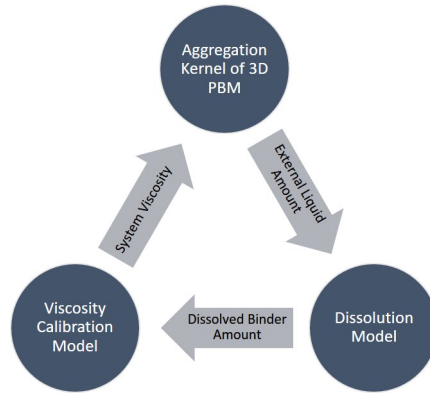


Figure 4.3: Integration of 1-D PBM and Dissolution Model using a viscosity calibration model

4.4 Drop Penetration

Hapgood et al. [12] studied the penetration of liquid drops into loosely packed powder beds and developed expressions for the calculation of drop penetration time for two different cases: constant drawing area (CDA) case and decreasing drawing area (DDA) case. It was seen that the drop penetration time depends linearly on the viscosity of the penetrating liquid. Since, the drop penetration time and thus rate of penetration of liquid into the particle affects external liquid content immensely, which in turn affects the viscosity of the system and consecutively the growth rate of particles, the dependence of drop penetration time on the viscosity was considered in this work. The viscosity of the wet binder solution added in case of wet binder addition is different for the two binders used and the viscosity drastically changes over time in the dry binder addition, the internal liquid content of the particle was formulated as a function of the inverse of viscosity. To account for the other parameters used in the expression by Hapgood et al. [12], multiple constant parameters such as the internal liquid drop penetration constant, compartment drop penetration constant and initial liquid spread constant were introduced.

4.5 Numerical Methods

The differential equations are solved simultaneously using first order explicit Euler integration technique which has been previously used for solving multi-dimensional PBM by [3, 8]. The selection of time step for integration is very crucial as it affects number of particles leaving and entering a particular size class at any time-step. If the time-step is very large, number of particles leaving the bin may be more than the number of particles present in that bin at that time-step. Hence a Courant-Friedrichs-Lewy (CFL) condition as mentioned in [29] is used which checks the above mentioned limitation. In the model, the particles are distributed into different discrete particle size bins. Using a linear grid to define a broad range of particle sizes requires a large number of bins, thereby increasing the computational expense of the model greatly. Therefore, a non-linear grid was designed as follows,

$$s_i = s_1 * (4.7)^{i-1} \quad (4.25)$$

where i represents the bin number in one dimension and s_1 indicate the solid volume of particle in the smallest bin. A cell average technique developed by [20] for 1-D PBM and by Chaudhury et al. [7] for 3-D PBM was applied to distribute the particles that are formed in the intermediate range of two bins, into the adjacent bins. This technique distributes these particles into surrounding bins based on the relative distances from the corresponding bins. The liquid and gas volume bins were lumped into the solid volume bins, and the average liquid and gas volume for each solid volume bin were calculated at each time-step. Values of the different parameters used in the model are shown in the table below.

Table 4.2: Process parameters, material properties used in simulation

Property/Parameter	Symbol	Model Value
Granulation time	t_{final}	1320 s
Volume of first bin, solid	s_1	$4.8 \times 10^{-13} \text{ m}^3$
Total number of bins	ns	14
Volume ratio of spray zone	α_1	0.3
Volume ratio of bulk zone	α_2	0.7
Liquid spray rate	U_{spray}	$5 \times 10^{-6} \text{ m}^3/\text{s}$
Granule density	den_s	$350 \text{ kg}/\text{m}^3$
Contact angle	θ	1.3 radian
HPC diffusion coefficient	D	$8.3 \times 10^{-9} \text{ m}^2/\text{s}$
PVP diffusion coefficient	D	$5 \times 10^{-9} \text{ m}^2/\text{s}$
Initial binder size	A_{init}	$49.375 \text{ }\mu\text{m}$
HPC saturation solubility	C_s	0.33
PVP saturation solubility	C_s	0.33
Diffusion layer thickness	h_i	$0.5 \text{ }\mu\text{m}$
Water density	den_l	$1000 \text{ kg}/\text{m}^3$

The computations were performed in MATLAB 2015b on an Intel(R) Core(TM) i7-4710HQ CPU (2.5GHz) with 16 GB RAM.

During the development of model, the system is discretized into different particle size bins which have their appropriate differential equation expressed in Equations 4.1 and 4.4. These equations are solved simultaneously using first order Euler integration technique which has been previously used for solving multi-dimensional PBM by Barrasso and Ramachandran [3] and Chaudhury et al. [8]. This explicit integration

technique track the population distribution with every time step. The selection of time step is very crucial as it determines number of particles leaving a particular size class. If the time step is very large, particles leaving the bin would be more than the number of particles present in that bin. Hence a Courant-Friedrichs-Lewy (CFL) condition as mentioned in [29] is used which checks the above mentioned limitation. The size ranges that are observed in an industrial granulation system is very large and hence a grid has to be designed to define these size classes. Since using a linear grid to define that broad range requires a large number of bins, a non-linear grid was designed as follows,

$$s_i = s_1 * (4.7)^{i-1} \quad (4.26)$$

where i represents the bin number in one dimension and s_1 indicate the solid volume of particle in the smallest bin. However, use of non-linear grid gives rise to some particle size which lie between the defined grids. To account for these particles, a cell average technique developed by [20] for 1-D PBM and by Chaudhury et al. [7] for 3-D PBM. This technique distributes these particles into surrounding bins based on the relative distances from the corresponding bins. The computations were performed in MATLAB 2015b on an Intel(R) Core(TM)i7-4710HQ CPU processor (2.5GHz) with 16 GB RAM.

Chapter 5

Results and Discussion

5.1 Granule growth in Dry & Wet HPC addition

Figure 5.1(a) shows the conservation of solid volume over the entire duration of granulation. As expected, the solid volume is constant over all the three stages of granulation namely pre-mixing, liquid addition and wet massing. Also, there is no liquid present in the system during the pre-mixing stage and the liquid volume increases during the liquid addition stage and reaches a maximum value at the end of liquid addition which is equal to the total liquid added to the system (Figure 5.1(b)). During the wet massing stage, the liquid volume remains constant with time.

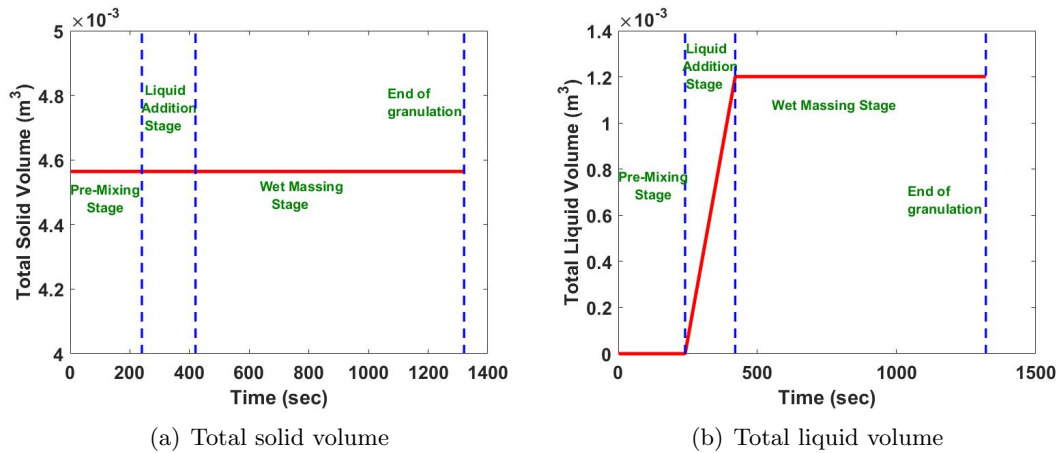


Figure 5.1: Conservation of total solid and liquid volumes over time

The dissolution of binder in the dry addition plays an important role since a faster dissolution leads to higher viscosity early on leading to higher growth. The amount of binder dissolved per unit volume of water or the concentration of binder solution in the system over time was also studied and is shown in Figure 5.2. It can be seen that the dissolution of binder does not start immediately when water is added. This

is in tune with the the assumption that the liquid added to the system first seeps into the pores of the particles. When the pores of the particles are completely filled internal liquid from the pores starts to come out and dissolve the binder. Since the spray zone receives higher amount of water than the bulk zone during liquid addition, binder dissolution for both compartment start at different time. Initially when amount of liquid is less, maximum binder dissolves to attain saturation leading to maximum viscosity in respective compartments. Since in the spray zone, the amount of binder present initially is less compared to the bulk zone, the binder solution concentration decreases more rapidly as more water is continuously added directly to the spray zone. In the bulk zone, the lesser amount of water present and the water transported from the spray zone due to particle circulation is not enough to dissolve the large amount of dry binder present. As a result, whatever water is present in the bulk zone remains saturated for some time even after liquid addition stops. After all of the binder gets dissolved, the viscosity starts to decrease because of the dilution of the saturated binder liquid with unsaturated, more dilute solution transferred from the spray zone due to particle circulation. Also, the internal liquid coming out of the pores due to consolidation of particles dilutes the binder solution even more. However, in the spray zone, the binder solution concentration starts to increase after the liquid addition stage because of the unsaturated binder solution moving *to* bulk zone *from* the spray zone and the saturated binder solution moving *to* spray zone *from* the bulk zone due to particle circulation. At each time-step, viscosity of both compartments are evaluated from the binder percentages by fitting the experimentally acquired viscosity-concentration curve (Figure 5.4) with a power law expression.

The presence of different viscosity regimes in the same system exists only in dry binder granulation which creates a significant difference between the WBA and DBA systems. Higher viscosity helps particles to stick to each other when they collide leading to faster growth, which is also represented by the Stokes criterion explained in the Appendix. The value of the aggregation kernel β_{agg} represented by Equation 4.12 changes based on the Stokes criterion. The increase in viscosity decreases the Stokes number of colliding particles resulting in aggregation provided that the Stokes number

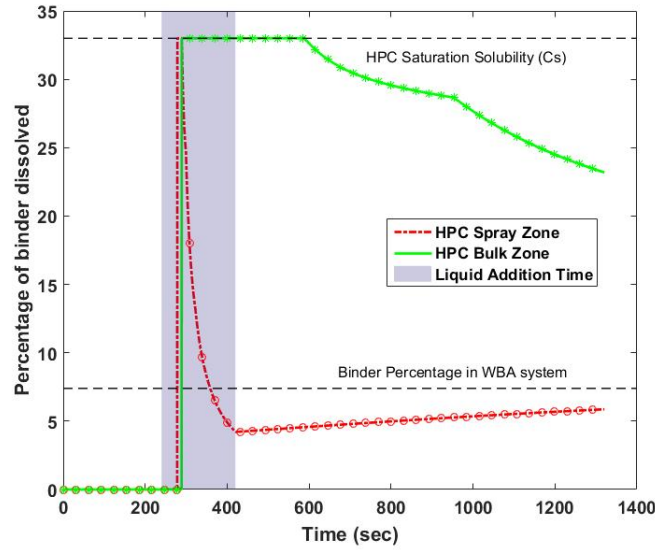


Figure 5.2: Variation of binder solution concentration with time for HPC in spray zone and bulk zone

is below a critical Stokes Number as shown in Equation A-4. As a result, particles have a bigger growth in the dry addition compared to the wet addition.

Figure 5.3 illustrates the experimentally observed and model predicted average diameter of granules with time for wet granulation with HPC. Figures 5.3(a) and 5.3(b) respectively show the dynamic evolution of average diameter for wet and dry addition of HPC. As the water added during dry binder addition is less viscous than the binder solution added during wet addition, the drop penetration rate is higher for the water. So, the water goes into the granule pores faster in dry addition than the binder solution in wet addition. As a result, the particle growth starts at the onset of liquid addition stage in wet addition because of the higher amount of external liquid present, which helps the particles stick to each other after collision. In contrast, for the dry addition, since the water goes into the pores very fast, there is no external liquid present to facilitate particle growth. In the absence of external liquid the binder particles also do not dissolve and create viscous liquid to help the particles grow. However, after some time of continuous liquid addition, the pores get filled with water and the additional liquid being added to the system stays on the particle surface and starts to dissolve the binder particles. Since, the amount of water available for the binder to dissolve in at this point

is very less, the resulting solution is saturated and significantly more viscous than the binder solution added in the case of wet addition. Therefore, the particles grow at a very fast rate which is higher than the growth rate in case of wet addition. We believe mainly due the higher viscosity in the case of dry addition, for reasons explained above, the particles also have a higher average diameter at the end of the process.

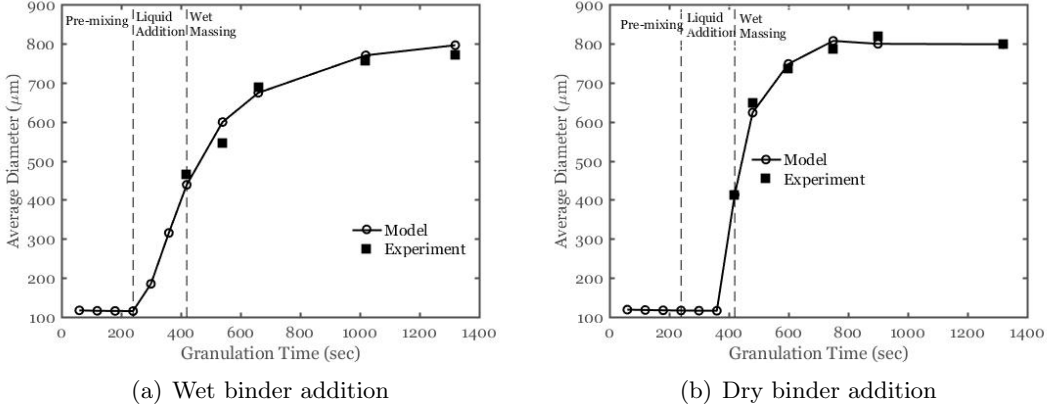


Figure 5.3: Experimental & model predicted average diameter for wet & dry addition of HPC

5.2 Granule growth in Dry & Wet PVP addition

The model developed for HPC binder system was also applied to another binder, PVP. As reported in literature, binder properties can greatly affect the granulation and granule properties [21]. The two binders used in this study, HPC and PVP, have different particle properties such as density, saturation solubility, diffusion coefficient which determines its dissolution rate in water. Moreover, they result in significantly different viscosities when they are dissolved in water as shown in Figure 5.4.

As can be seen from the Figure 5.4, HPC has a higher viscosity compared to PVP for the same binder solution concentration. Also the saturation solubility for HPC (33% (wt/wt)) is higher than the saturation solubility of PVP (10% (wt/wt)). As a result the more of the HPC can dissolve in the water producing a binder solution with considerably higher viscosity compared to PVP.

The model successfully captures the viscosity difference in spray and bulk zone for

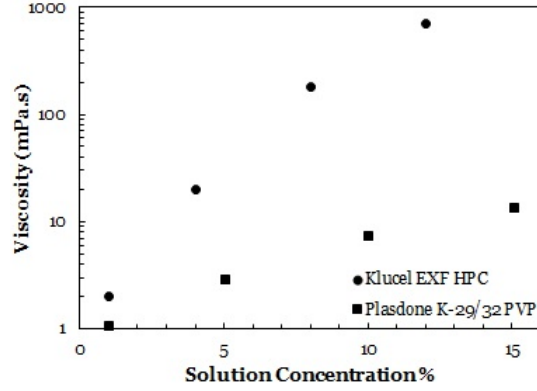


Figure 5.4: Correlation of viscosity with binder concentration in water

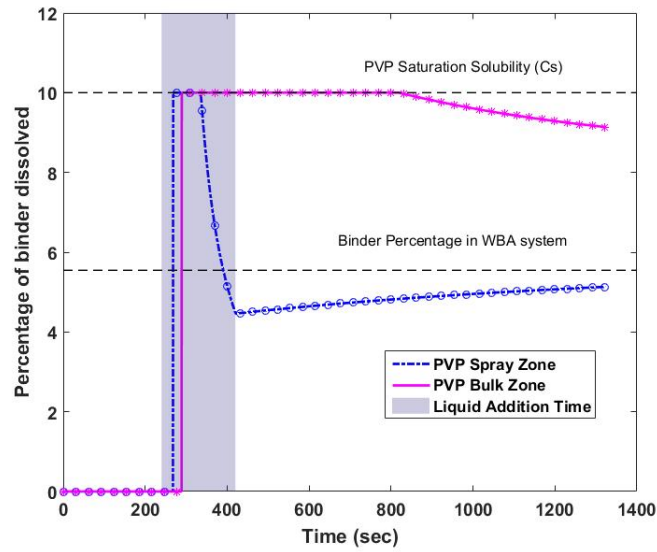


Figure 5.5: Variation of binder solution concentration with time for PVP in spray zone and bulk zone

PVP dry addition system as shown in Figure 5.5. Similar to HPC dry addition, the spray zone gets high amount of liquid directly during liquid addition. Therefore, once all the binder in the spray zone is dissolved, and the saturation concentration is reached, the dilution of binder solution starts and the binder solution concentration in the spray zone reduces rapidly. On the other hand, the bulk zone receives less amount of liquid and the high amount of binder present in this zone saturates the liquid. After the liquid addition is stopped, the circulation of particles with unsaturated binder solution from spray zone and saturated binder solution from bulk zone reduces the difference between the binder solution concentration in the two zones. It is important to note that the

bulk zone binder solution concentration remains at the saturation concentration for a longer period in case of PVP compared to HPC (Figure 5.2). This happens since the saturation solubility concentration of PVP is less than that of HPC.

Figure 5.6 shows the experimentally observed and model predicted average diameter with time for wet granulation with PVP. Figures 5.6(a) and 5.6(b) respectively represent wet and dry addition of PVP. PVP behave a little differently from the HPC binder due to the difference in dissolution rate between those. Due to the faster dissolution PVP in water in case of dry addition, the binder solution becomes very viscous right at the start of the liquid addition stage. The binder solution for dry addition being more viscous than the binder solution added in wet addition, penetrates slowly into the pores of the particles. This results in higher amount of external liquid which is also more viscous, in the case of dry addition compared to wet addition. Therefore, the particles grow very fast in dry addition right from the start of liquid addition. However, since PVP dissolves in water quickly the binder solution in dry addition become similar to the binder solution in wet addition in terms of concentration. This results in similar viscosities for both the case, resulting in almost identical growth rate. Similar to HPC, the particles attain a slightly higher diameter in case of dry addition.

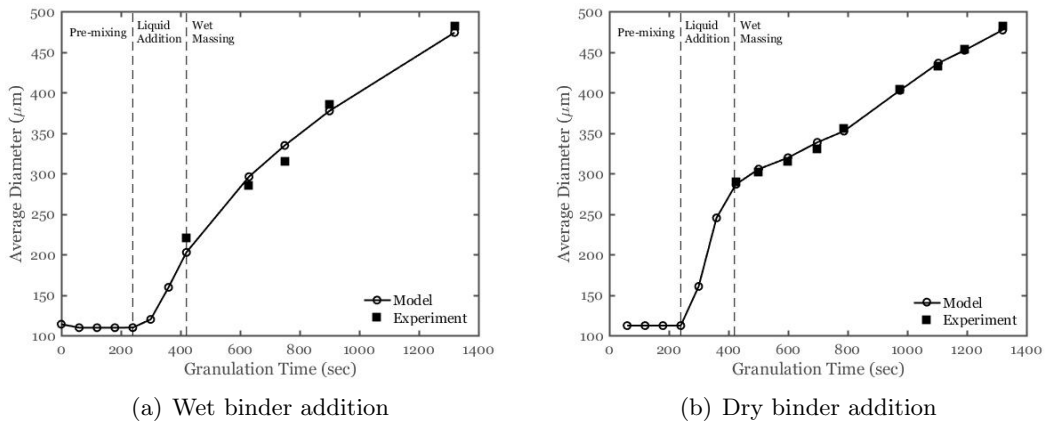


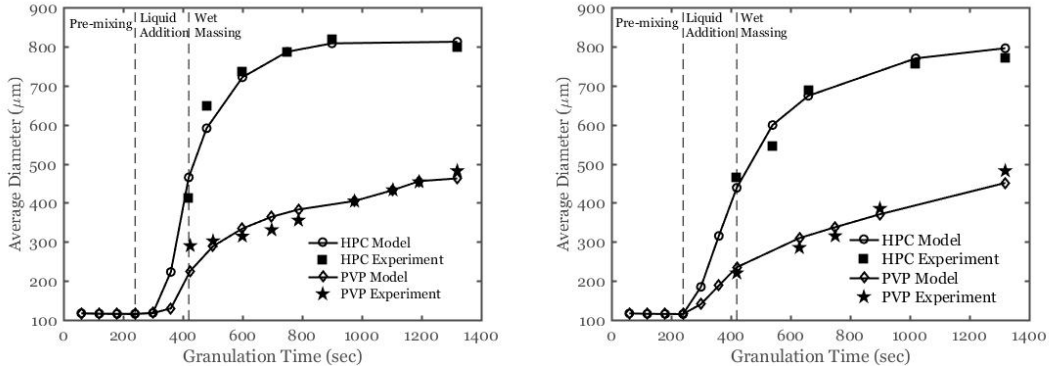
Figure 5.6: Experimental & model predicted average diameter for wet & dry addition of PVP

It is important to note that the difference between the final average diameter in wet and dry addition of HPC is higher than that of PVP. This can be attributed to the fact

that the rate of change of viscosity with binder concentration is considerably higher in case of HPC. As a result, the difference between the wet and dry addition systems, which is mainly due to their difference in viscosity is higher in case of HPC than PVP.

5.3 Sensitivity Analysis

The model uses different process kernels that depend on various parameters as shown in Table 4.2. These parameters define the rates of aggregation, breakage, consolidation and binder dissolution which further control the granule size during granulation. Sensitivities of these parameters on granulation is studied by offsetting their values in six different levels between -30% to +30% and measuring the percentage change in average diameter at start and end of wet massing time. Figure ?? illustrates the effect of changing these factors on average diameter of granules. It can be observed that some parameters such as binder size and density, diffusion coefficient, contact angle and circulation rate have the least effect on granule diameter at both wet massing times. The granule saturation and liquid addition rate have higher impact on diameters at the start of wet massing time than at the end which is supported by the hypothesis that these parameters affect the rate of binder dissolution which prominently affects the aggregation at early stages of wet massing time. The collision force between two granules and granules with the granulator affect the rates of aggregation, breakage and consolidation. This force is majorly by the impeller diameter and rotational speed and hence these factors affect the granule diameter remarkably both at start and end of wet massing stage as demonstrated in Figures ?? and ?. The binder solubility also determines the binder dissolution and hence affects the granules at an early stage. Finally, the minimum porosity and granule density also have notable effect, as these affect consolidation, a key rate process of granulation. Analysis of the sensitivities of all these factors helps to understand the rate processes and provide control over granulation output.



(a) Model *calibration* with *dry* binder addition of HPC & PVP (b) Model *prediction* for *wet* binder addition of HPC & PVP

Figure 5.7: Prediction of wet binder addition by calibrating the model with dry binder addition

5.4 Prediction of wet binder addition from dry binder addition

Once the model was found to be capable of reproducing the behavior of the dry and wet addition systems for both binders, it was used to predict the average diameter of the wet binder addition systems for both binders. The model uses an empirical breakage kernel, semi-mechanistic aggregation kernel and binder dissolution sub-model and drop penetration calculation along with consolidation and liquid addition calculations which have various parameters such as aggregation constant, breakage constant, consolidation constant, rpm-consolidation constant, minimum porosity, circulation rate constant, internal liquid drop penetration constant, compartment drop penetration constant and initial liquid spread constant that needs to be estimated. The numerical values of these parameters used in this model was obtained by fitting the model with experimental average particle diameter (d_{50}) for dry addition of HPC and PVP. With the estimated parameters from the dry addition cases, the average diameter of the wet addition cases over time for both HPC and PVP were predicted. The accuracy of the fits with experimental data were measured using the sum of squared errors (SSE) as expressed in Equation 5.1.

$$SSE = \sum_{n=1}^N \left(\frac{d_{50_{expn}} - d_{50_{simn}}}{d_{50_{expn}}} \right)^2 \quad (5.1)$$

where, n represents different granulation times at which samples were collected. The SSE for the two calibration sets and the two prediction sets are provided in the table below.

Table 5.1: Sum of squared errors in the model predicted average diameter for the estimated parameters

Case	Used for	SSE
HPC dry Addition	Calibration	0.001
PVP dry Addition	Calibration	0.003
HPC wet Addition	Prediction	0.001
PVP wet Addition	Prediction	0.002

Chapter 6

Conclusion

Development of multi-compartment model for high shear granulation with wet addition of binder has been typically done for the past years to understand the heterogeneity involved in this process. From this analysis, it can be seen that with the inclusion of dry binder addition as a factor, the heterogeneity increases. The dry binder addition includes a binder dissolution process in addition to the rate processes observed in wet binder addition. In this work, a mathematical model is developed to study the dynamics of binder dissolution process in dry binder granulation. Good agreement between model and experimental data suggests that the binder gradually dissolves in liquid and its rate is influenced by the liquid volume and the saturation solubility. This gives rise to a dynamic viscosity environment in granulator, changing with time. The rate processes, owing to the changing viscosity, also are affected accordingly thereby affecting granule growth. These rate mechanism defined by PBM is integrated with dissolution model to identify the dynamics of DBA. Integrating the dissolution model with multi-compartmental population balance model adds more complexity and requires high computational power to solve it. Here, we developed a reduced ordered model with only two compartments, one for high viscosity condition and other for low viscosity condition, and combined it with dissolution sub-model. This model is computationally less intensive and can account for heterogeneity in process and also predict the final d_{50} (average diameter) of granule with good accuracy.

The model supports the experimental observations that in dry binder addition system the growth rate of granules is higher than wet binder system. The viscosity and liquid volume are the main factors contributing for this observed difference. These two factors prominently changes the aggregation and breakage process which directly affects

the granule size. In addition to these factors, the granulation also depends on other parameters which can affect the granule growth. Sensitivity analysis of the model showed that the process parameters such as diameter and rotational speed of impeller and liquid addition rate and material properties such as granule density, minimum porosity of granule, granule saturation constant have significant effect on granule size. The model was further applied to the granulation involving PVP binder with dry and wet addition. A new set of parameter values were determined for this binder system and the model was successful in predicting similar trends for granule growth with respect to experimental data.

This study provides a good understanding of rate processes involved in granulation with dry binder addition. The model developed in this work can be used to predict granule distribution at the end of wet massing time by varying the input parameters such as initial particle size distribution, rotational speed of impeller, liquid addition rate within a defined design space. The parameter values can be optimized in a wider design space for further application of this model to granulation with binders of different properties.

Bibliography

- [1] Dana Barrasso and Rohit Ramachandran. A comparison of model order reduction techniques for a four-dimensional population balance model describing multi-component wet granulation processes. *Chemical Engineering Science*, 80:380–392, 2012. ISSN 00092509. doi: 10.1016/j.ces.2012.06.039.
- [2] Dana Barrasso and Rohit Ramachandran. Chemical Engineering Research and Design Multi-scale modeling of granulation processes : Bi-directional coupling of PBM with DEM via collision frequencies. *Chemical Engineering Research and Design*, 93(April):304–317, 2014. ISSN 0263-8762. doi: 10.1016/j.cherd.2014.04.016.
- [3] Dana Barrasso and Rohit Ramachandran. Qualitative Assessment of a Multi-Scale , Compartmental PBM-DEM Model of a Continuous Twin-Screw Wet Granulation Process. *Journal of Pharmaceutical Innovation*, 2015. ISSN 1872-5120.
- [4] Dana Barrasso and Rohit Ramachandran. Multi-scale modeling of granulation processes: Bi-directional coupling of {PBM} with {DEM} via collision frequencies. *Chemical Engineering Research and Design*, 93:304 – 317, 2015.
- [5] C. A. Biggs, C. Sanders, A. C. Scott, A. W. Willemse, A. C. Hoffman, T. Instone, A. D. Salman, and M. J. Hounslow. Coupling granule properties and granulation rates in high-shear granulation. *Powder Technology*, 130(1-3):162–168, 2003. ISSN 00325910. doi: 10.1016/S0032-5910(02)00260-7.
- [6] I. T. Cameron, F. Y. Wang, C. D. Immanuel, and F. Stepanek. Process systems modelling and applications in granulation: A review. *Chemical Engineering Science*, 60(14):3723–3750, 2005. ISSN 00092509. doi: 10.1016/j.ces.2005.02.004.

- [7] Anwesha Chaudhury, Avi Kapadia, Anuj V. Prakash, Dana Barrasso, and Rohit Ramachandran. An extended cell-average technique for a multi-dimensional population balance of granulation describing aggregation and breakage. *Advanced Powder Technology*, 24(6):962 – 971, 2013. ISSN 0921-8831. doi: <http://dx.doi.org/10.1016/j.appt.2013.01.006>.
- [8] Anwesha Chaudhury, Huiquan Wu, Mansoor Khan, and Rohit Ramachandran. A mechanistic population balance model for granulation processes: Effect of process and formulation parameters. *Chemical Engineering Science*, 107:76 – 92, 2014.
- [9] Anwesha Chaudhury, Marco Euclide Armenante, and Rohit Ramachandran. Compartment based population balance modeling of a high shear wet granulation process using data analytics. *Chemical Engineering Research and Design*, 95:211–228, 2015. ISSN 02638762. doi: 10.1016/j.cherd.2014.10.024.
- [10] Anders Darelus, Anders Rasmuson, and Ingela Niklasson Bjo. High shear wet granulation modelling a mechanistic approach using population balances. 160: 209–218, 2005.
- [11] Anders Darelus, Henric Brage, Anders Rasmuson, Ingela Niklasson Björn, and Staffan Folestad. A volume-based multi-dimensional population balance approach for modelling high shear granulation. *Chemical Engineering Science*, 61(8):2482–2493, 2006. ISSN 00092509. doi: 10.1016/j.ces.2005.11.016.
- [12] Karen P. Hapgood, James D. Litster, Simon R. Biggs, and Tony Howes. Drop penetration into porous powder beds. *Journal of Colloid and Interface Science*, 253(2):353 – 366, 2002. ISSN 0021-9797. doi: <http://dx.doi.org/10.1006/jcis.2002.8527>.
- [13] Karen P. Hapgood, James D. Litster, and Rachel Smith. Nucleation regime map for liquid bound granules. *AIChE Journal*, 49(2):350–361, 2003. ISSN 00011541. doi: 10.1002/aic.690490207.
- [14] M. J. Hounslow, J. M. K. Pearson, and T. Instone. Tracer studies of high-shear

- granulation: II. population balance modeling. *AIChE Journal*, 47(9):1984–1999, 2001. ISSN 1547-5905. doi: 10.1002/aic.690470910.
- [15] Charles David Immanuel and Francis Joseph Doyle III. Solution technique for a multi-dimensional population balance model describing granulation processes. *Powder Technology*, 156(23):213 – 225, 2005. ISSN 0032-5910. doi: <http://dx.doi.org/10.1016/j.powtec.2005.04.013>. Particle Technology Forum Special Issue Papers presented in the Particle Technology Forum sessions at the 2003 Annual {AIChE} meeting in San Francisco (November, 2003) Papers presented in the Particle Technology Forum sessions at the 2003 Annual {AIChE} meeting in San Francisco (November, 2003).
- [16] Simon M. Iveson. Limitations of one-dimensional population balance models of wet granulation processes. *Powder Technology*, 124(3):219–229, 2002. ISSN 00325910. doi: 10.1016/S0032-5910(02)00026-8.
- [17] Simon M. Iveson, James D. Litster, Karen Hapgood, and Bryan J. Ennis. Nucleation, growth and breakage phenomena in agitated wet granulation processes: A review. *Powder Technology*, 117(1-2):3–39, 2001. ISSN 00325910.
- [18] K.A. Kusters. The influence of turbulence on aggregation of small particles in agitated vessels. *Ocean Engineering*, 1991. ISSN 00298018. doi: 10.1016/0029-8018(79)90021-0.
- [19] Timo Kulju, Marko Paavola, Horst Spittka, Riitta L Keiski, Esko Juuso, Kauko Leiviskä, and Esa Muurinen. Modeling continuous high-shear wet granulation with DEM-PB. *Chemical Engineering Science*, 142:190–200, 2016. ISSN 0009-2509.
- [20] J. Kumar, M. Peglow, G. Warnecke, S. Heinrich, and L. Mrl. Improved accuracy and convergence of discretized population balance for aggregation: The cell average technique. *Chemical Engineering Science*, 61(10):3327 – 3342, 2006. ISSN 0009-2509. doi: <http://dx.doi.org/10.1016/j.ces.2005.12.014>.
- [21] J J Li, L Tao, M Dali, D Buckley, J Gao, and M Hubert. The Effect of the Physical States of Binders on High-Shear Wet Granulation and Granule Properties: A

- Mechanistic Approach Towards Understanding High-Shear Wet Granulation Process. Part I. Physical Characterization of Binders. *Journal of pharmaceutical sciences*, 100(1):164–173, 2011. ISSN 00223549. doi: Doi10.1002/Jps.22260.
- [22] Jianfeng Li, Ben Freireich, Carl Wassgren, and James D. Litster. A general compartment-based population balance model for particle coating and layered granulation. *AIChE Journal*, 58(5):1397–1408, 2012.
- [23] J D Litster, S E Pratsinis, and B J Ennis. Powder Technology Population balance modelling of drum granulation of materials with wide size distribution. 82:37–49, 1995.
- [24] Huolong Liu and Mingzhong Li. Two-compartmental population balance modeling of a pulsed spray fluidized bed granulation based on computational fluid dynamics (CFD) analysis. *International Journal of Pharmaceutics*, 475(1-2):256–269, 2014. ISSN 0378-5173. doi: 10.1016/j.ijpharm.2014.08.057.
- [25] David L. Ma, Danesh K. Tafti, and Richard D. Braatz. Optimal control and simulation of multidimensional crystallization processes. *Computers & Chemical Engineering*, 26(78):1103 – 1116, 2002.
- [26] L Madec, L Falk, and E Plasari. Modelling of the agglomeration in suspension process with multidimensional kernels. *Powder Technology*, 130(13):147 – 153, 2003. ISSN 0032-5910. doi: [http://dx.doi.org/10.1016/S0032-5910\(02\)00258-9](http://dx.doi.org/10.1016/S0032-5910(02)00258-9).
- [27] S.J. Maronga and P. Wnukowski. Establishing temperature and humidity profiles in fluidized bed particulate coating. *Powder Technology*, 94(2):181 – 185, 1997.
- [28] Hideya Nakamura, Hiroyuki Fujii, and Satoru Watano. Scale-up of high shear mixer-granulator based on discrete element analysis. *Powder Technology*, 236:149–156, 2013. ISSN 0032-5910.
- [29] Rohit Ramachandran and Paul I. Barton. Effective parameter estimation within a multi-dimensional population balance model framework. *Chemical Engineering*

- Science*, 65(16):4884 – 4893, 2010. ISSN 0009-2509. doi: <http://dx.doi.org/10.1016/j.ces.2010.05.039>.
- [30] Rohit Ramachandran and Anwesha Chaudhury. Model-based design and control of a continuous drum granulation process. *Chemical Engineering Research and Design*, 90(8):1063 – 1073, 2012.
- [31] S. Shanmugam. Granulation techniques and technologies: recent progresses. *Bioimpacts*, 5(1):55–63, 2015.
- [32] Miroslav Soos, Jan Sefcik, and Massimo Morbidelli. Investigation of aggregation, breakage and restructuring kinetics of colloidal dispersions in turbulent flows by population balance modeling and static light scattering. *Chemical Engineering Science*, 61(8):2349 – 2363, 2006. ISSN 0009-2509. doi: <http://dx.doi.org/10.1016/j.ces.2005.11.001>.
- [33] H.S. Tan, M.J.V. Goldschmidt, R. Boerefijn, M.J. Hounslow, A.D. Salman, and J.A.M. Kuipers. Building population balance model for fluidized bed melt granulation: lessons from kinetic theory of granular flow. *Powder Technology*, 142(23):103 – 109, 2004. ISSN 0032-5910. doi: <http://dx.doi.org/10.1016/j.powtec.2004.04.030>.
- [34] Daan Verkoefen, Gerard A. Pouw, Gabriël M. H. Meesters, and Brian Scarlett. Population balances for particulate processes - A volume approach. *Chemical Engineering Science*, 57(12):2287–2303, 2002. ISSN 00092509. doi: 10.1016/S0009-2509(02)00118-5.
- [35] Jianzhuo Wang and Douglas R. Flanagan. General solution for diffusion-controlled dissolution of spherical particles. 1. theory. *Journal of Pharmaceutical Sciences*, 88(7):731–738, 1999. ISSN 1520-6017. doi: 10.1021/js980236p.

Appendix

Aggregation has a significant impact on final granule properties during granulation. The aggregation process is further affected by operating parameters such as impeller speed, amount of liquid and binder properties such as viscosity, density, contact angle. Hence an aggregation kernel that includes these parameters can facilitate the understanding of system behavior.

According to the semi-mechanistic kernel developed by [8], the aggregation kernel can be represented as a product of stokes criterion and fractional wetted area.

$$K_{agg}(s, l, g, s-s', l-l', g-g') = B_0 \Psi(s, l, g, s-s', l-l', g-g') * A(s, l, g, s-s', l-l', g-g') \quad (\text{A-1})$$

where $A(s, l, g, s-s', l-l', g-g')$ is the fractional wetted area and $\Psi(s, l, g, s-s', l-l', g-g')$ is the stokes criterion which depicts the stokes criterion for aggregation and can be calculated from Stokes criterion as in Equation A-2.

Stokes Criterion

The Stokes criterion represents the probability of aggregation based on the stokes number of colliding particles. If this value is less than a critical value, then the colliding particles will agglomerate whereas if this value is higher than the critical value, it indicates there is no aggregation.

$$\Psi(s, l, g, s-s', l-l', g-g') = \begin{cases} 1 & St \leq St^* \\ 0 & St \geq St^* \end{cases} \quad (\text{A-2})$$

where St is the stokes value of colliding particles and St^* is the critical stokes value which are defined as follows

$$St = \frac{8\tilde{m}u_0}{3\pi\mu\tilde{d}^2} \quad (\text{A-3})$$

$$St^* = 2ln \frac{\lambda_{12}}{h_a} \quad (\text{A-4})$$

Here, \tilde{d} and \tilde{m} are the harmonic means of diameter and mass of aggregating particles respectively, u_0 is velocity and μ is viscosity of the particles. h_a is the surface asperity of the particle which is assumed to be in the range of 2% of the particle diameter to a maximum of 3 μm . λ_{12} is the depth of surface liquid on particles that facilitates aggregation and can be expressed as a function of liquid volume and wetted area.

$$\lambda_{12} = 1.5 \frac{V(t, s, l, g)}{A_{wet}(s, l, g)} \quad (\text{A-5})$$

During granulation, liquid added to the system comes in contact with the particles and goes into the pores till saturation. With time, excess liquid due to liquid addition and consolidation accumulate on the surface increasing the wetted radius which can be represented as a function of contact angle, θ

$$R_{wet} = \frac{3V}{\pi} \phi(\theta) \quad (\text{A-6})$$

where,

$$\phi(\theta) = \frac{\sin^3(\theta)}{2 - 3\cos(\theta) + \cos^3(\theta)} \quad (\text{A-7})$$

and the volume of external liquid is

$$V(t, s, l, g) = l * (1 - x^*) \quad (\text{A-8})$$

where x^* is the granule saturation fraction and l is the amount of liquid associated with the granule. The total liquid associated with the particle is categorized into internal liquid and external liquid. While, the external binder liquid involves in the aggregation, the internal liquid does not have any part in this process.

Fractional wetted area

The factor $A(s, l, g, s - s', l - l', g - g')$ represents the product of fractional wetted area of the two aggregating particles and can be expressed as

$$A(s, l, g, s - s', l - l', g - g') = \frac{A_{wet}(s, l, g)}{A_{total}(s, l, g)} * \frac{A_{wet}(s - s', l - l', g - g')}{A_{total}(s - s', l - l', g - g')} \quad (\text{A-9})$$

In A-9, A_{wet} is the area of granule covered by binder solution and A_{total} is the total area of granule.